

# Confinement Hoops of Compression Zone in Beam under Cyclic Loading

*by* Nuroji Nuroji

---

**Submission date:** 14-Sep-2019 04:21PM (UTC+0700)

**Submission ID:** 1172520263

**File name:** 6.\_Confinement\_hoops\_of\_compression\_zone\_in.pdf (1.05M)

**Word count:** 2850

**Character count:** 13582

# Confinement Hoops of Compression Zone in Beam under Cyclic Loading

Yulita Arni Priastiwi<sup>1, a)</sup>, Iswandi Imran<sup>2, b)</sup>, Nuroji<sup>1, c)</sup> and Arif Hidayat<sup>1, d)</sup>

## INTRODUCTION

Ductile structure is an absolute requirement for the earthquake resistant structures design, especially for areas with high earthquake zones [1]. However, to obtain a ductile structure must be supported by structural elements that are also ductile. This is because structural elements with high ductility will be able to maintain their strength after undergoing considerable inelastic deformation without having to collapse. The ductile structural elements will be able to larger rotation, and maintain their energy dissipation capability and also will absorb more energy to ensure the ongoing mechanism of plastic joints in predetermined places [2].

Plastic hinge regions of beam needs special attention, especially in column face while receiving sizeable negative moment by both gravity and the added due to earthquake load. When an earthquake, the compression zone of beam's must hold the enough large negative moment and shear while usually compression concrete area is very small so prone to collapse. This research it intended a more ductile structure elements in the plastic hinge region of beam by providing confinement in compression zone of beam's section.

Past research on the confinement especially regarding confinement in the compression zone of beam's have shown that the existence of confinement in compression zone of beam's be able to improve ductility of beam [3] and hoops-shaped confinements provide good results in increasing ductility of the beam when given monotonic loading

[4] on specimens depicting the plastic hinge on beam region.

The continuation of the study was developed by reviewing similar specimen models with cyclic loading. Beam specimen behavior which is a simplification of the plastic hinge area of the beam in front of the column with

additional confinement hoops in the compression zone will be subjected to cyclic loading that represents the earthquake load received by the structure element.

16 The beam is designed with a tensile and compressive reinforcement equal ratio then compared to the beam without confinement in the compression zone. The loading of a centralized load in the center of 15 the beam span is intended to allow the specimen to receive the largest moment and shear as well as the area of the plastic hinge in the face of the column. This research is important because research on the confinement in the compression zone of beam's especially in the plastic hinge region very limited, whereas in designed structures of resistant earthquake, plastic hinge precisely localized in beam at column face and the bottom of the columns leg in 1st floor with the intention that the structure can able to dissipate seismic energy very well.

## EXPERIMENTAL DETAILS

The experimental study is aimed to simulate plastic hinges of beam at column face, where the beam has remained to have enough ductility in bending though shear exist. In this research use two 150 mm x 300 mm x 4000 mm reinforced concrete (RC) beams with enlargement at the mid-span to represent column in structure has been tested. These beams supported by simply support with 3600 mm span and loaded by reversal single point loading at midspan, so that the beam subjected to bending moment and also shear at the column face. To avoid eccentricity, the both supports joint and roller located in line to the beam axis with cylindrical and oval hole inserted by 50 mm diameter rod bar.

The beam subjected to incremental loading through hydraulic actuator, and displacement in the mid span is measured by using Linear Variable Displacement Transducer (LVDT) that record displacement of every increment loading. LVDT is also installed horizontally on the top and bottom of the column face to measure the curvature that occurs between them.

### Reinforcement Detail

Both of the specimens have the same tension and compression longitudinal steel bars i.e. 2D22. These have done because the beam section would receive a tensile and compressive loads alternately. The specimens can be distinguished in RC beam without confinement named BNS as a control beam and RC beam with extra confinement shaped of hoops D10-70 in the compression zone named BCS with confinement reinforcement ratio ( $\rho_{cf}$ ) = 5.38%.

Longitudinal bars are continued along the beam and bent 90° with minimum hook length  $12d_b$  [5], as well stirrups and confining bars were bent 135° with length of hook  $6d_b$  ( $d_b$  was the diameter of the bar). In addition to the main longitudinal reinforcement D22 was also installed longitudinal reinforcement  $\phi 6$  as the confinement holder. On both specimens the first stirrup to prevent shear failure was located at 50 mm from column face. The dimension of enlargement was 250 mm x 400 mm at mid-span that called stub to simulate column, with the stiffness more large compared the beam. The reinforcement in stub was used 14D16 providing a reinforcement ratio of 2.81% the gross section of the stub and used stirrup D10-50. Thus as a result of the imposition, maximum moment of beam was localized 5 column face to form plastic hinge and observation be focused in this area. Whereas confinement hoops will be installed on the top and bottom of the beam because both sides of beam will be compression area alternately due to cyclic loading.

Confinement hoops measuring 110 x 90 mm that made of reinforcement deform D10 with 70 mm spacing between confinements. Confinement hoops n3 mounted alternating with stirrup for shear was also within 70 mm. The first position of the confinement hoops at a distance of 85 mm from the face of the stub and the following next distance was 70 mm from the first confinement.

In the hole support area of joint or roller were given a layer of steel pipe with the thickness  $\pm 3$  mm with diameter hole of 2 in (50.8 mm) corresponding with holes made on the concrete and strengthened by cross reinforcement. It was intended to avoid direct contact between solid steel and concrete, as well as to prevented possible things from causing damage to the area. Detail of reinforcement for the specimen BCS and BNS shown in Fig 1.

### Properties of Materials

The longitudinal and shear reinforcement in this study used deformed-bars except additional longitudinal steel bar  $\phi 6$  in BCS use plain bars to embed confinement reinforcement. The result tensile test of bars D22, D16 and

D10 were 476 MPa, 402 MPa and 444 MPa respectively, while the tensile strength of plain bar  $\phi 6$  was 430 MPa. In this study, the specimen using normal strength concrete with the composition of concrete mix / m<sup>3</sup> was shown in Table 1. The concrete mix with a slump value of 100 mm was used Ordinary Portland Cement Type I, which used for general usability, while the sand and coarse aggregate used local products.

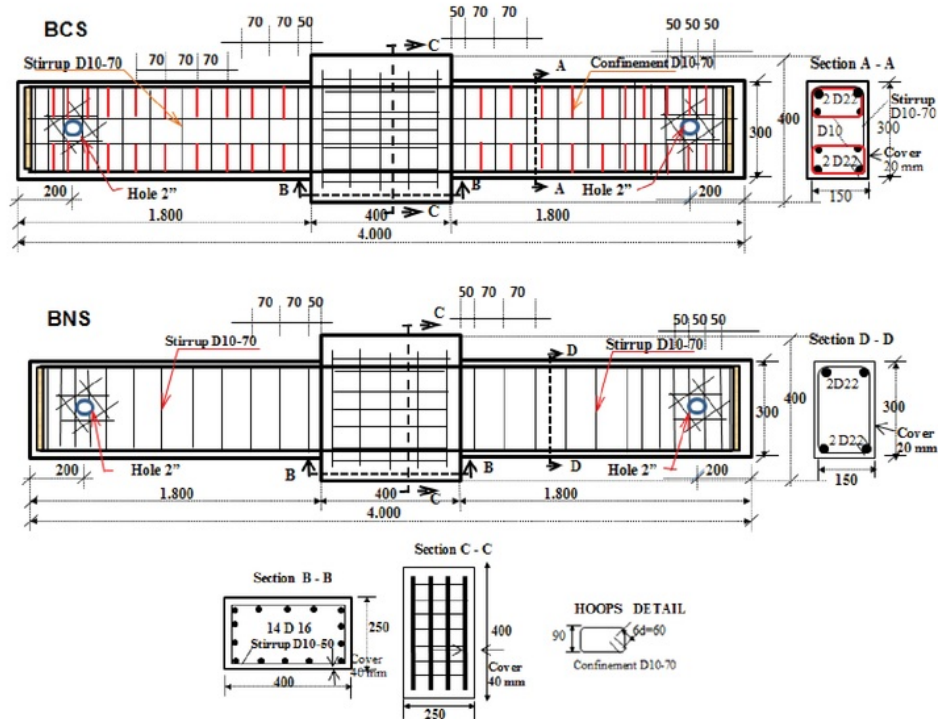


FIGURE 1. Details of specimen reinforcement at BCS and BNS

Concrete mix also used fly ash type F which is a waste of burning bituminous coal with CaO content of less than 10%. It was intended to reducing the amount of cement and replace with fly ash of 25% by weight of cement. To improving the workability at the time of casting, was used superplasticizer Plastiment V50 type with a dose of 0.25% by weight of cement. Coarse aggregate use the maximum grain size of 9.5 mm with the intention that the aggregate coarse grain can through between reinforcement in order to avoid the porous of the concrete.

TABLE 1. Proportion of concrete materials

Material	Weight (Kg/m <sup>3</sup> )	Volume (%)
Cement Type I	331	13.76
Fly Ash Type F	83	3.45
Coarse Aggregate	982	40.83
Fine Aggregate	787	32.73
Superplasticiser Plastiment V50	0.84	0.03
Water	221	9.19
Totl Weight/m3	2405	100



## Set up and Instrumentation

The beam specimens are placed on the test frame which is strongly crossed on the rigid floor. The specimen beam support on the center to obtain the same neutral axis between the tensile and compressive the concrete cross section. Steel plate measuring 350 x 400 mm with a thickness of 20 mm is placed attached not only to the top side of the stub but also on the underside. Both of plates united with the specimens and connected with eight pieces of steel bars with a diameter of 25 mm as a binder.

Hydraulic actuator and load cell of similar capacity 500 kN are used to provide centralized cyclic-loading at center of the beam span. Some LVDTs were used to measure vertical displacement of beam at midspan and near both supports to maintain control that were fixed vertically, and the other LVDTs were fixed horizontally at the both side column on top and bottom of beam to measure curvature of beam at the column face. Both the load cell or LVDT and also strain gauge are connected to the data logger or the data recorder. The experimental setup shows in Fig 2. To measuring strain of steel bar and concrete, some strain gauges were attached on surface of bars and concrete. Fig 3 shows the location of strain gauges on the concrete and reinforcement in specimens.

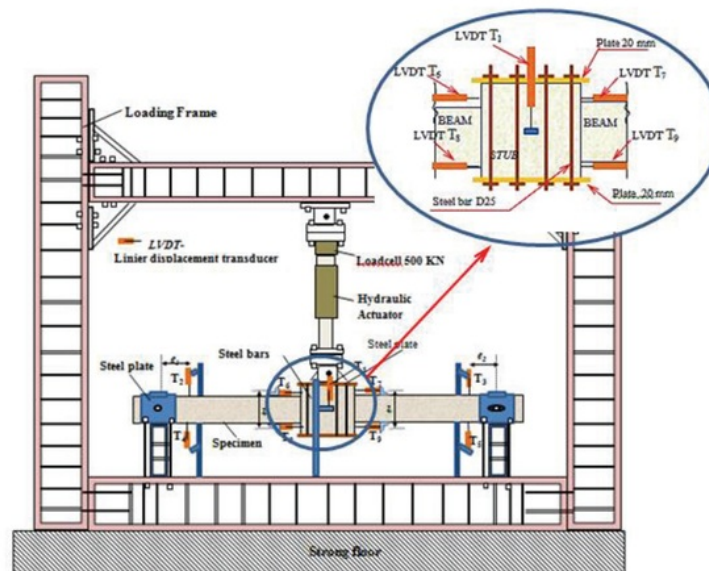


FIGURE 2. Experimental set up

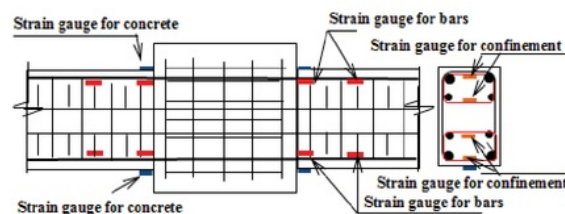


FIGURE 3. Strain gauge location

The cyclic loading on the BNS and BCS provided by the displacement control system with the model of quasi static cyclic loading which is a technique loading that was applied gradually and slowly enough, so that the influence of dynamic inertia and the effect of strain rate on the material is negligible. Standard tests conducted by the ACI 374.1-05 (Acceptance Criteria for Moment Frames Based on Structural Testing and Commentary)[6] with a

load sequence consisting of three cycles for each level drift ratio (DR) starts from DR 0.2% and so on until they reached ultimate conditions such as shown in Fig 4.

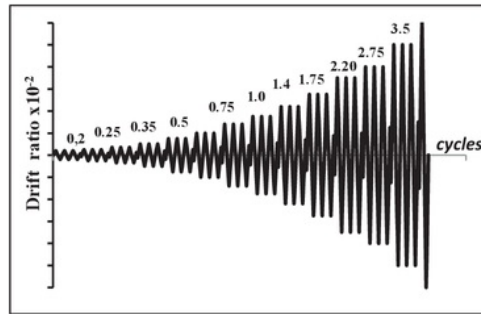


FIGURE 4. Loading cycles based ACI 374.1-05[6]

## RESULT AND DISCUSSION

7

Test results in both specimens at the end of the test showed that the specimen has a behavior with hysteresis curve shape was good. Hysteresis curve showed that the beam's failure of the dominant bending and the plastic hinge formation at the site of the planned in front of the stub. At every drift level for three cycles provided no strong degradation strength or stiffness. This shows that the detailing of specimens in accordance with the given standards.

Hysteresis curve from the results of the LVDT vertical readings at mid-span showed that up to its collapse BNS were able to experience 36 cycles of testing at DR= 5% and BCS able to experience 40 cycles of testing at DR 6%. The relationship graph of load-drift ratio of the test results is shown in Fig 5.

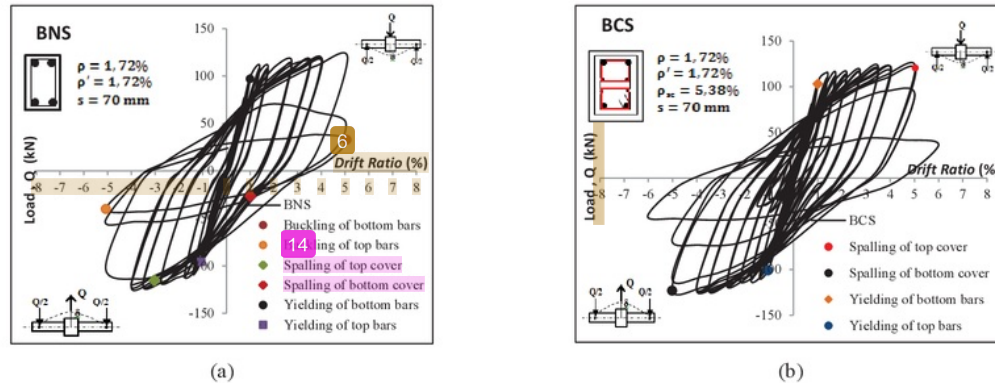


FIGURE 5. (a) Hysteresis curve of BNS (b) Hysteresis curve of BCS

1

The specimens BNS was designed as beam without additional confinement in compression zone has good resistance to cyclic loading cycles up to 33rd in the drift ratio of 4%, but then began to occur degradation stiffness when entering a cycle of 34th both tensile loading or compression which is then followed by a load drop significantly. While the BCS curve which is a beam with confinement hoops in compression zone is shown that the specimen was able to maintain its strength stably until the 38th cycle of drift ratio of 5% both on tensile loading and the compression, but when entering 39th cycle started strength and stiffness degradation occurs both on tensile loading or compressive exceed 20% of maximum force that occurs. At BCS test is discontinued after a rapid decrease in the load on the 40th cycle. The milestone of BNS and BCS testing experimental shown at Table 2.

The depiction of the moment-curvature curve obtained from the readings of horizontal LVDT were placed on top and bottom of the beam at z distance from each other so far. The hysteresis curve generated from the horizontal LVDT was then converted into the average envelope curve of two-direction loading to determine the value of the

yield as  $w_3$  as ultimate value. The magnitude of plastic hinge moment for the area searched by  $M = (Q / 2 * L_a)$ , where  $L_a$  is the distance between support to face of stub. The curvature found using horizontal displacement data LVDT  $\Delta_c$  on top ( $\Delta_c$ ) and bottom ( $\Delta_s$ ) which is divided by length in the first instance to get the value of strain  $\epsilon_c$  and  $\epsilon_s$ . Then from the strain distribution above and below, curvature be sought by  $\phi = (\epsilon_c + \epsilon_s)/z$ . Fig 6 shows the moment vs. curvature relationship graph. To determine the value of ductility displacement ( $\mu_\Delta$ ) and curvature ductility ( $\mu_\phi$ ) in this study refers to the method used by Bayrak and Sheikh [7], while Table 3 shows the summary of test results.

TABLE 2. History loading at BNS and BCS

History	BNS (at kN)	BCS (at kN)
Spalling of top cover	-115.3	120.5
Spalling of bottom cover	-26.5	-123.1
Yielding of top bars	-101.2	-101.2
Yielding of bottom bars	96.9	103
Buckling of top bars	-40.1	Not happen
Buckling of bottom bars	32.7	Not happen

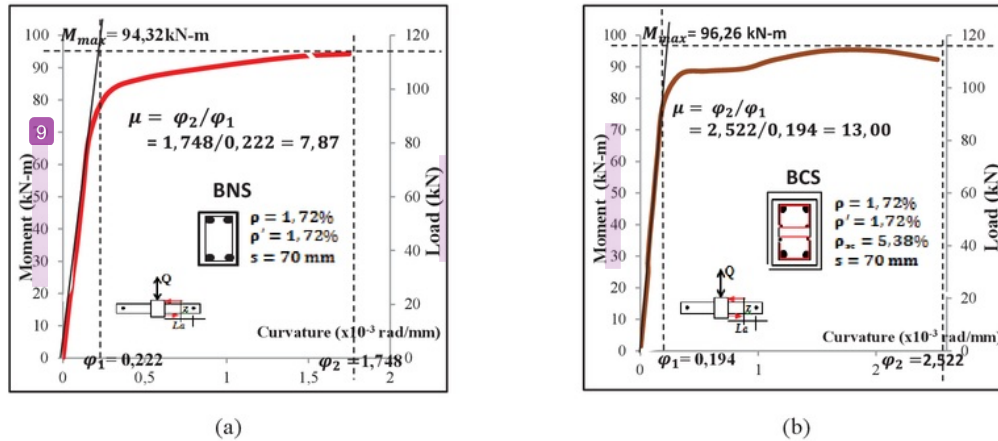


FIGURE 6. Moment-curvature graph on (a) BNS (b) BCS

The graph in Fig 6(a) and Fig 6(b) shows that the curvature ductility value ( $\mu$ ) which is obtained from the ratio of the ultimate curvature ( $\phi_2$ ) and the yield curvature ( $\phi_1$ ), BCS was greater than BNS of 13.00 and 7.87. The graph also shows when the maximum moment between the two specimens is not much different that is 94.32 and 96.26 kN-m for BNS and BCS respectively.

Table 3 shows an increase ductility displacement and ductility curvature reach 50 up to 65% and the cumulative displacement ( $N_\Delta$ ) which aims to see the value cumulative inelastic displacement that occurs in the test object increase 79% at BCS compared BNS. To demonstrate the energy dissipation characteristics of the beam was also calculated the value of W (Index cumulative energy dissipation), where from the test results increased more than two times.

TABLE 3. Summary of test result

Result	Specimen		Increase BCS to BNS (%)
	BNS	BCS	
Qmax (kN)	117.9	120.33	2.06
Mmax (kN-m)	94.32	96.26	2.06
$\mu_\Delta$	3.01	4.52	50.4
$\mu_\phi$	7.87	13	65.1
$N_\Delta$	35.8	64.11	79.08
W(x108)	8.62	28.36	229

## <sup>1</sup> CONCLUSION

<sup>1</sup>  
Based on the experimental results of cyclic tests, the specimen beam added with confinement in the compression zone is capable of behaving more ductile than the beam without additional confinement in the compression zone. Beams are still capable of developing displacement and curvatures even though there has been no increase in the capacity nor the moment. The existence of a confinement in the beam cross section of the beam can extend the load cycle experienced by the specimen due to cyclic loading. The extent of the hysteresis curve due to cyclic loading on the beam with the confinement in the compression zone shows a more stable curve than a beam without confinement.

The presence of confinement in the compression zone of beam is able to significantly increase the ductility of the beam that is 50% to 65, but is less significant at the increase in the moment and load capacity that is 2.06 %. To cyclic loading, the presence of confinement in the compression zone of the beam also increases the ability of the beam in terms of energy dissipation. This can be seen from the increase of cumulative energy dissipation index value (W) which increased more than 200%.

## ACKNOWLEDGMENTS

Special gratitude is expressed to LPPM Diponegoro University on research funding through research grant scheme RPP (Riset Pengembangan dan Penerapan).



# Confinement Hoops of Compression Z one in Beam under Cyclic Loading

## ORIGINALITY REPORT

16%

SIMILARITY INDEX

7%

INTERNET SOURCES

11%

PUBLICATIONS

5%

STUDENT PAPERS

## PRIMARY SOURCES

- |   |   |    |
|---|---|----|
| 1 | Yulita Arni Priastiwi, Iswandi Imran, Nuroji, Arif Hidayat. "Behavior of Ductile Beam with Addition Confinement in Compression Zone", Procedia Engineering, 2014<br>Publication                                       | 4% |
| 2 | <a href="http://eprints.undip.ac.id">eprints.undip.ac.id</a><br>Internet Source   | 3% |
| 3 | Priastiwi, Yulita Arni, Iswandi Imran, and Nuroji. "The Effect of Different Shapes of Confinement in Compression Zone on Beam's Ductility Subjected to Monotonic Loading", Procedia Engineering, 2015.<br>Publication | 2% |
| 4 | <a href="http://aip.scitation.org">aip.scitation.org</a><br>Internet Source   | 1% |
| 5 | <a href="http://www.tandfonline.com">www.tandfonline.com</a><br>Internet Source   | 1% |
| 6 | <a href="http://www.cuee.titech.ac.jp">www.cuee.titech.ac.jp</a><br>Internet Source   | 1% |

7	Submitted to Asian Institute of Technology Student Paper	1 %
8	Advances in FRP Composites in Civil Engineering, 2011. Publication	1 %
9	Eric T. Visage, Brad D. Weldon, David V. Jauregui, Craig M. Newtson. "Flexural Performance of Ultrahigh-Performance Concrete Developed Using Local Materials", Journal of Materials in Civil Engineering, 2019 Publication	1 %
10	Submitted to Universiti Putra Malaysia Student Paper	1 %
11	Liang Huang, Chen Zhang, Libo Yan, Bohumil Kasal. "Flexural behavior of U-shape FRP profile-RC composite beams with inner GFRP tube confinement at concrete compression zone", Composite Structures, 2018 Publication	<1 %
12	theses.ucalgary.ca Internet Source	<1 %
13	Submitted to University of Greenwich Student Paper	<1 %
14	Ilias Gkimousis, Vlasios Koumousis. "Modeling RC column flexural failure modes under	<1 %

# intensive seismic loading", Earthquake Engineering & Structural Dynamics, 2018

Publication

15

Submitted to Kingston University

Student Paper

<1%

16

Heba A. Mohamed. "Improvement in the Ductility of Over-reinforced NSC and HSC Beams by Confining the Compression Zone", Structures, 2018

Publication

<1%

Exclude quotes Off

Exclude matches Off

Exclude bibliography Off